

Effects of Shell on Bore-center Annular Shaped Charges Formation and Penetrating into Steel Targets

Wenlong Xu[#], Cheng Wang^{*,*}, Jianming Yuan[@], Weiliang Goh[@], and Bin Xu[#]

[#]State Key Laboratory of Explosion Science and Technology, Beijing Institute of Technology, Beijing - 100 081, China

[@]Nanyang Technological University, 50 Nanyang Drive - 637 553, Singapore

^{*}E-mail: wangcheng@bit.edu.cn

ABSTRACT

Annular shaped charge can efficiently create large penetration diameter, which can solve the problem of small penetration diameter of a traditional shaped charge, and thus meeting the requirements of large penetration diameter in some specific situations. In this paper, the influence of five kinds shell structures, i.e. no shell, aluminum shell with thickness of 2.0 mm and steel shell with thickness of 2.0 mm, 3.0 mm and 4.0 mm, on bore-center annular shaped charges (BCASCs) formation and penetrating steel targets was investigated by numerical simulations and experiments. The numerical simulation results are in good agreement with the experimental results. The results showed that, from no shell to aluminum shell of 2.0 mm and then to steel shell of 2.0 mm, 3.0 mm and 4.0 mm for BCASCs, the diameter and radial velocity of projectile head decrease, the axial velocity of BCASC projectiles increases gradually, the penetration diameter of the targets decreases, and the penetration depth increases. The penetration diameter caused by the BCASC with no shell is the largest, being 116.0 mm (1.16D), D is the charge diameter. The penetration depth caused by the BCASC with steel shell of 4.0 mm thickness is the deepest, being 76.4 mm (0.76D).

Keywords: Annular shaped charge; Shell; Numerical simulation; Penetration

1. INTRODUCTION

The shaped charge has important application in civil and military fields^{1,2}. However, the traditional shaped charge has small penetration hole diameter, which can't satisfy the demand for large diameter in specific occasions, such as emergency rescue, oil exploitation, tandem warheads, and so on. The annular shaped charge can quickly and efficiently create large penetration diameter, so it has attracted wide attention of scholars, and a variety of annular shaped charge structures had been designed^{3,4}.

The idea of cylindrical shape of penetrator was first mentioned in 1970⁵. This shape of penetrator allows to increase the hole diameter in the target. The shaped charge with W-like liner, probably, for the first time was considered by V.F. Minin⁶, *et al.* It was shown that circular shaped charge jet may be formed due to collapsing of W liner. Later, this mechanism was described by them^{7,8}. Moreover, they proposed that well-known theory of jet formation by Birkhoff can't apply to shaped charge liners with high collapsing angles (which take place in W-like liners)⁹. Wang¹⁰, *et al.* investigated a W-like annular shaped charge and proposed the design principle of it. They found not all W-type annular shaped charge can form annular jets, only the designed W-type liner, which fulfils the "equal impulse of inner and outer liner wall" has the capability

of forming stable annular jet. Minin¹¹, *et al.* proposed another mode of W-liner which can form explosive pulsed plasma antennas for information protection. The performances of explosive ordnance disposal between annular projectiles and classical EFP with constant mass were compared by Rondot¹². A clear decrease of energy and pressure levels in the explosion were observed when using a reasonably designed annular projectile. The simulation results of impacting explosive shown that the inner diameter of the annular projectile should be large enough to limit overpressure by recombination of the shock waves. Grace and Barnard¹³ designed a dual-mode annular shaped charge which can produce reconstituted and tubular jets using a single charge geometry by simply varying the initiation radius of the explosives. The results shown that, when the initiation take place near the pole radius, a tubular jet will be formed. To form a reconstituted jet, the initiation needs to take place near the periphery of the explosive. In recent years, some novel shaped charges, for example swept and axilinear shaped charges, which can cause super caliber hole have been designed by Innovative Defense company¹⁴.

In this paper, based on the BCASCs charge structure designed in our previous work¹⁵, the influence of shell on its forming and penetration into steel target was investigated by combining numerical simulations with penetration experiments.

2. EXPERIMENTS

2.1 Experimental Scheme

Structures of BCASC are as shown in Fig. 1. It is composed of a copper annular liner, composition B explosive and a shell. Composition B explosive consists of 40% TNT and 60% RDX. The diameter D of composition B explosive and liner is 100.0 mm, and the center of liner has a hole with diameter $d=4.0$ mm. As shown in Fig. 2, the outer surface (contact surface with explosive) section of the liner is two semicircles with radius $R_1=24.0$ mm and the distance between the centers of the two semicircles is $d'=52.0$ mm. The inner wall section of the liner was two interior arcs which were less than half circle with radius $R_2=21.7$ mm. The height of composition B explosive and shell is $L=180.0$ mm. The following shell conditions (a) no shell ($K=0.0$ mm), (b) aluminum shell ($K=2.0$ mm) and (c) steel shell ($K=2.0$ mm, 3.0 mm and 4.0 mm), were used to study the BCASCs, where K refers to the thickness of the shell.

The experimental setup of different shell conditions is as shown in Fig. 3. The paper standoff cylinder was used between BCASCs and steel targets, and the standoff distance is 100.0

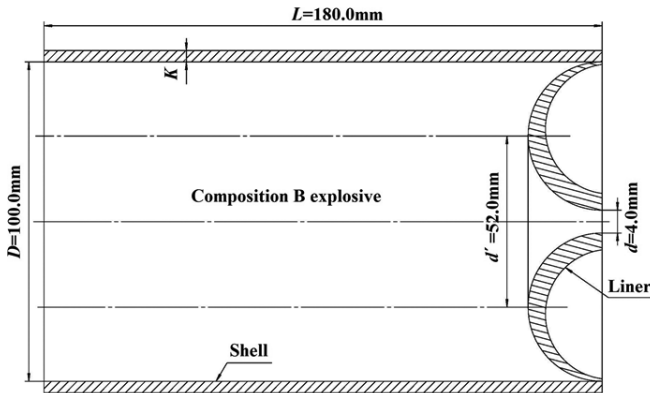


Figure 1. Schematic of the BCASC.



Figure 2. Annular liners used in the experiments.

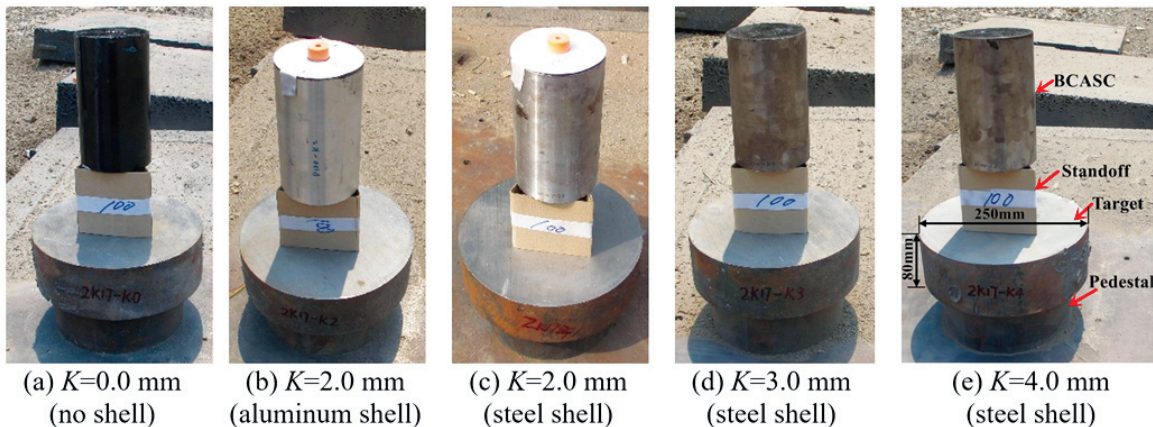


Figure 3. Experimental setup.

mm (1.0D). The steel target is cylindrical with a diameter of 250.0 mm and height of 80.0 mm. The steel target is supported by steel pedestal.

2.2 Experimental Results and Discussions

As shown in Fig. 4, BCASC of the five shell conditions can create an approximate circular bullet holes with a core in the center of the bullet holes. The diameter of core formed by no shell and aluminum shell BCASC penetrating targets is larger than that formed by BCASCs with steel shell. As shown in Fig. 4(e), when the shock waves propagate in the target, due to the influence of the interface, the target produces tensile damage and radial fracture. In the axial direction of the target, no obvious spallation phenomenon is observed on the back of the target due to the supporting effect of the steel pedestal. The upper surface of the cores penetrated by BCASCs with steel shell ($K=3.0$ mm and 4.0 mm) was severely damaged and had lower height than that of other targets. From no shell to aluminum shell of 2.0 mm and then to 2.0 mm, 3.0 mm and 4.0 mm steel shell of BCASCs, the penetration diameter of the targets decreases, and the penetration depth increases. As listed in Table 1, for all the five shell conditions, when $K=0.0$ mm (no shell), the penetration diameter of the entrance is the largest, being 116.0 mm (1.16D), and the penetration depth is the smallest, which is 30.0 mm (0.30D). When $K=4.0$ mm (steel shell), the penetration diameter of the entrance is the smallest, being 87.3 mm (0.87D), but the penetration depth is the largest, which is 76.4 mm (0.76D).

3. NUMERICAL SIMULATIONS

3.1 Numerical Methods

The AUTODYN remap method was used in the numerical simulation. Firstly, a two-dimensional axisymmetric Euler model (see Fig. 5) of the BCASC was established. The size of the air region of the model is 400 mm×160 mm, and the

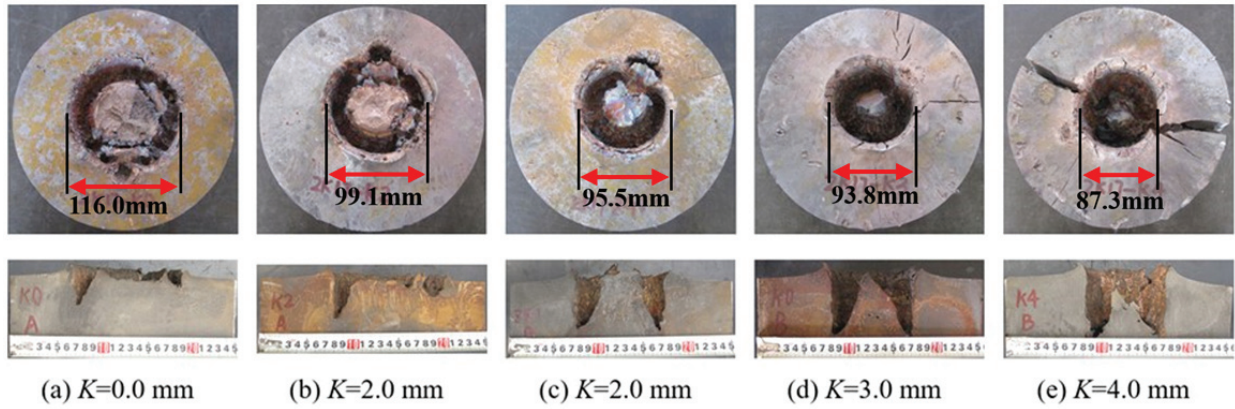


Figure 4. Experimental results of penetration steel targets under different shell conditions.

Table 1. The values of penetration holes

Measured parameters	Parameter variable (mm)				
	$K=0.0$ mm (no shell)	$K=2.0$ mm (aluminum shell)	$K=2.0$ mm (steel shell)	$K=2.0$ mm (steel shell)	$K=2.0$ mm (steel shell)
Entrance diameter	116.0	99.1	95.5	93.8	87.3
Penetration depth	30.0	48.0	56.6	64.7	76.4

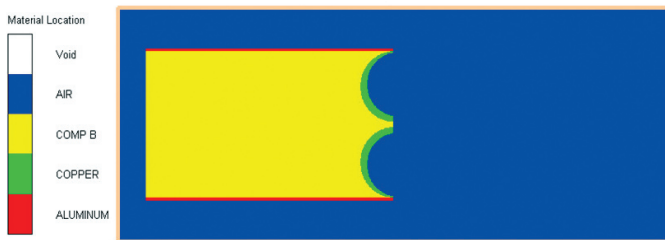


Figure 5. Initial formation model of BCASC with aluminum shell.

boundary condition of air is the flow-out. In the second step, Lagrange grid of BCASC penetrating steel target was established, and the results of BCASC formation were mapped to the target model (see Fig. 6). According to the comparison between numerical simulation and X-ray experiments¹⁵, mesh sizes of $0.4\text{ mm} \times 0.4\text{ mm}$ were used for both Euler and Lagrange model.

In the numerical simulations, the ideal gas equation of state (EoS) and JWL EoS were used to describe the air and composition B explosive, respectively. The EoS of the liners, shells and targets (copper, aluminum and steel materials) was shock model. The strength of aluminum and steel materials was Johnson-Cook equation. The data used in the numerical simulations are from the AUTODYN material library¹⁶.

3.2 Numerical Results and Discussions

At $0.5D$ and $1.0D$ standoff distance, the numerical simulation results of BCASC with different shell conditions are as shown in Fig. 7. For the same standoff distance, from no shell to aluminum shell of 2.0 mm and then to steel shell of 2.0 mm, 3.0 mm and 4.0 mm for BCASCs, the diameter of projectile's head decreases gradually. With the increase of standoff distance, the head diameter of projectiles formed by BCASCs with no shell and aluminum shell increase, and

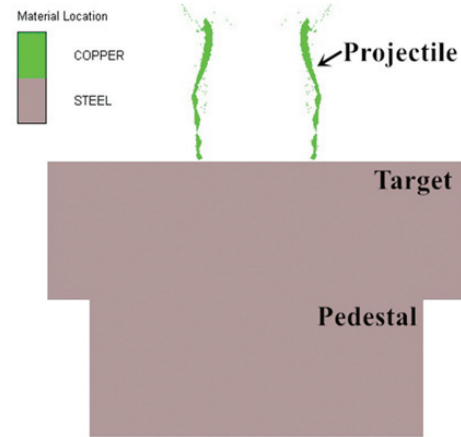


Figure 6. Model of BCASC with aluminum shell penetrating steel target.

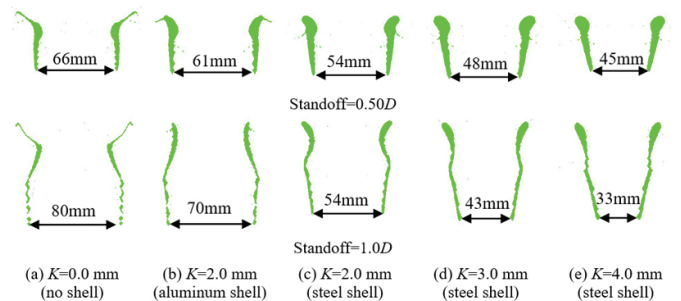


Figure 7. The projectiles formed by BCASC under various standoff distances and shells.

the diameter of the projectile's head is much larger than the distance of the outer wall centers of liner ($d'=52.0\text{ mm}$). The head diameter of projectiles formed by BCASCs with steel shell of 2.0 mm thickness does not change with the standoff distance. With the increase of standoff distance, the head diameter of projectiles formed by BCASCs with steel shell of

3.0 mm and 4.0 mm decreases. Consistent with the findings of Grace and Barnard¹², when the standoff distance increases to a certain value, the projectiles' head formed by BCASCs with steel shell of 3.0 mm and 4.0 mm will collapse in axis of symmetry, firstly.

At $0.5D$ standoff distance, the radial velocity of the projectiles formed by BCASCs with different shell conditions is shown in Fig. 8. The radial velocity of the projectile's tail formed by BCASCs with no shell and aluminum shell is less than zero, and the projectile's tail will deflect to the axis of the charge. Along the measuring line from tail to head of the projectile, the radial velocity of the projectile formed by BCASCs with no shell and aluminum shell increases first and then decreases slightly. The radial velocity of the projectile formed by BCASCs with steel shell first decreases, then increases and then decreases. From no shell to aluminum shell of 2.0 mm and then to steel shell of 2.0 mm, 3.0 mm and 4.0 mm, for projectile's head, the radial velocity decreases gradually. The radial velocity of the projectile's head formed by BCASCs with no shell and aluminum shell is greater than zero. So, the projectile's head will deflect away from the axis of the charge. The radial velocity of the projectile's head formed by BCASCs with steel shell of 2.0 mm thickness is slightly less than zero, and it is greater than zero in the middle of the projectile. The radial velocity of the projectile's head formed by BCASCs with steel shell of 3.0 mm and 4.0 mm thickness is less than zero, meaning the projectile's head will deflect to the axis of the charge, and the distance of the projectile's head will decrease gradually with the increase of the standoff distance.

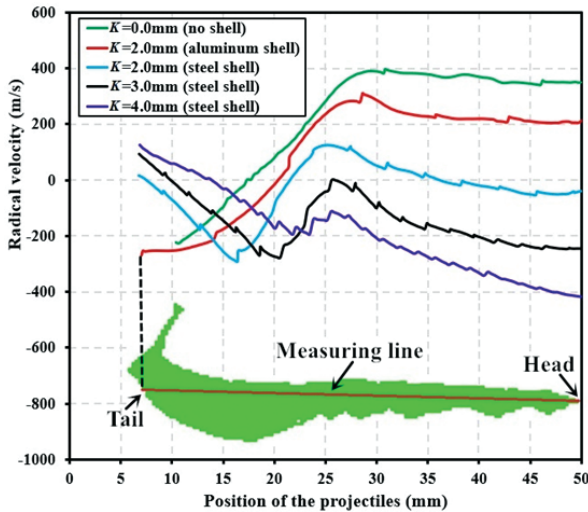


Figure 8. The radial velocity of the projectiles formed by BCASCs with different shell conditions ($0.5D$ standoff distance).

At $0.5D$ standoff distance, the axial velocity of the projectile formed by BCASCs with different shell conditions is shown in Fig. 9. For different shell conditions, from tail to head, the axial velocities of the projectile increase. When the coordinate position of measuring line is larger than 25 mm, from no shell to aluminum shell of 2.0 mm and then to steel shell of 2.0 mm, 3.0 mm and 4.0 mm of BCASCs, the axial velocity of projectile's head increases gradually. The axial

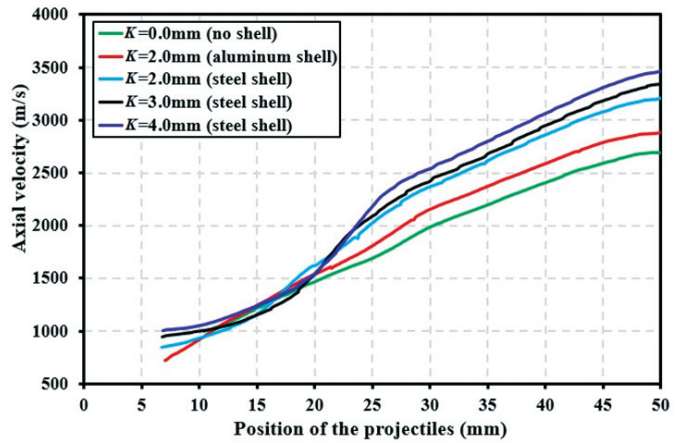


Figure 9. The axial velocity of the projectile formed by BCASCs with different shell conditions ($0.5D$ standoff distance).

velocity of the projectile's head formed by BCASC with no shell is the minimum, being 2691.3 m/s. The axial velocity of the projectile's head formed by BCASC with steel shell of 4.0 mm thickness is the largest, being 3463.0 m/s.

The simulation results of BCASC penetrating steel targets are shown in Fig. 10. From no shell to aluminum shell of 2.0 mm and then to 2.0 mm, 3.0 mm and 4.0 mm steel shell of BCASCs, the variation of penetration diameter and depth of numerical simulation results are in good agreement with the experimental results. Among all the shell conditions, the deviation between numerical simulations and experiments of BCASCs with aluminum shell of 2.0 mm thickness penetrating into steel targets is the largest, being 9.4%. Since the radial velocity of the projectile's tail formed by BCASCs with no shell and aluminum shell is directed to the charging axis, and the radial velocity of the projectile's head is away from the charging axis, the tail of the projectile cannot be coaxially penetrated along the head pre-opening hole. In addition, the axial velocity of the projectile formed by BCASCs with no shell and aluminum shell is low, so the penetration depth of them is small. As shown in Fig. 10 (a-b), when $t=0.07$ ms, the tail and head of the projectile break under the action of radial velocity gradient, and the fractured tail of the projectile impacts on the upper surface of the target core. In the penetration process, the radial position difference between the head and tail of the projectile formed by BCASC with steel shell of 2.0 mm thickness is smaller than that of other shell conditions. When $t=0.07$ ms, the tail of the projectiles formed by BCASCs with steel shell of 3.0 mm and 4.0 mm thickness impacts on the outer wall of the penetrating holes.

4. CONCLUSIONS

In this work, experiments and numerical simulations for BCASCs with no shell, aluminum shell and steel shell formation and penetrating steel targets were performed. The influence of shell conditions on the BCASCs formation and penetrating steel targets was investigated. From no shell to aluminum shell of 2.0 mm and then to steel shell of 2.0 mm, 3.0 mm and 4.0 mm for BCASCs, the diameter and radial velocity of the projectile head decrease, the axial velocity of BCASC

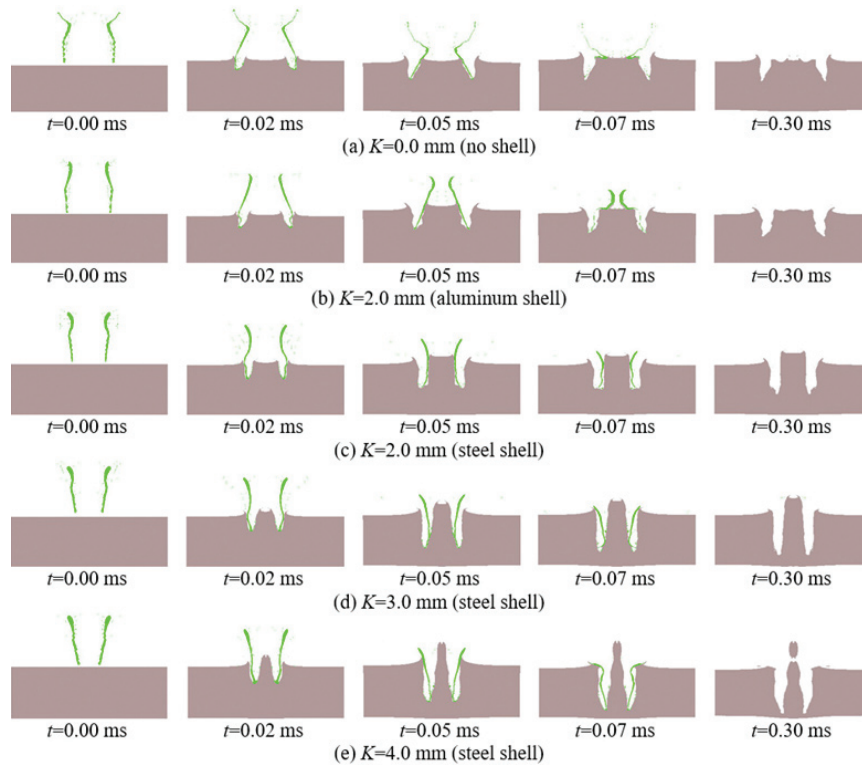


Figure 10. The numerical simulation results of BCASC penetrating steel targets.

projectiles increases gradually, the penetration diameter of the targets decreases, and the penetration depth increases. The penetration diameter created by the BCASC with no shell is the largest, being. The largest penetration depth of 76.4 mm ($0.76D$) is caused by the BCASC with steel shell of 4.0 mm thickness.

REFERENCES

- Wang, C.; Ding, J.X. & Zhao, H.T. Numerical simulation on jet formation of shaped charge with different liner materials. *Def. Sci. J.*, 2015, **65**(4), 279-286. doi: 10.14429/dsj.65.8648
- Wang, C.; Xu, W.L. & Yuen, S.C.K. Penetration of shaped charge into layered and spaced concrete targets. *Int. J. Impact Eng.*, 2018, **112**, 193-206. doi: 10.1016/j.ijimpeng.2017.10.013
- Leidel, D.J. A design study of an annular-jet charge for explosive cutting. Drexel University, 1978. PhD Thesis.
- Xu, W.L.; Wang, C. & Xu, B. Investigation of new type annular shaped charge formation mechanism. *Trans. Beijing Inst. Technol.*, 2018, **38**(6), 572-578 (Chinese). doi: 10.15918/j.tbit.1001-0645.2018.06.004
- Cable, A.J. High-impact phenomena. Edited by Kinslow, Academic Press, New York, USA, 1970. pp. 1-18.
- Minin, V.F.; Minin, I.V. & Minin, O.V. Principle of the forced jet formation. In Workshop air defense lethality enhancements and high velocity terminal ballistics: freiburg, Germany, 1998.
- Minin, V.F.; Minin, I.V. & Minin, O.V. Calculation experiment technology, computational fluid dynamics technologies and applications. Edited by Igor Minin, In Techopen, 2011. pp. 1-28.
- Minin, V.F.; Minin, I.V. & Minin, O.V. Some possibilities of hypercumulative regime of jet formations. *Appl. Mech. Mater.*, 2015, **782**, 42-48. doi: 10.4028/www.scientific.net/AMM.782.42
- Minin, V.F.; Minin, I.V. & Minin, O.V. Hypervelocity fragment formation technology for ground-based laboratory tests. *Acta Astronaut.*, 2014, **104**(1), 77-83. doi: 10.1016/j.actaastro.2014.07.027
- Wang, C.; Huang, F. & Ning, J. Jet formation and penetration mechanism of W typed shaped charge. *Acta Mech. Sinica*, 2009, **25**(1), 107-120. doi: 10.1007/s10409-008-0212-8
- Minin, I.V. & Minin, O. V. Explosive pulsed plasma antennas for information protection. In Advanced Microwave and Millimeter Wave Technologies Semiconductor Devices Circuits and Systems, Edited by Moumita Mukherjee, In Tech, 2010. pp. 13-34.
- Rondot, F.A. Computational parametric study on cookie-cutter projectiles. In 29th International Symposium on Ballistics: Edinburgh, Scotland, UK, 2016.
- Grace, F. & Barnard, M. Tubular and reconstituted jets using annular shaped charge liners. In 30th International Symposium on Ballistics: Long beach, CA, USA, 2017.
- Innovative defense super caliber charges. <http://innovativedefense.net/super-caliber-charges.php> (Accessed on 22 May 2019).
- Xu, W.L.; Wang, C. & Chen, D.P. Formation of a bore-center annular shaped charge and its penetration into steel targets. *Int. J. Impact Eng.*, 2019, **127**, 122-134. doi: 10.1016/j.ijimpeng.2019.01.008
- AUTODYN material library, ANSYS R17.2, ANSYS Inc., 2016.

ACKNOWLEDGMENTS

This research is supported by the National Natural Science Foundation of China (No. 11732003 and U1830139), Beijing Natural Science Foundation (No. 8182050), Science Challenge Project (No. TZ2016001), National Key R&D Program of China (No.2017YFC0804700) and the project of State Key Laboratory of Explosion Science and Technology (Beijing Institute of Technology). The opening project number is KFJJ20-10M.

CONTRIBUTORS

Dr Wenlong Xu received his PhD from Beijing Institute of Technology, in 2018. Presently working as a post-doctoral at Nanyang technological university. His area of research is explosion mechanics.

In current study, he performed the simulations and experiments and analysed the results obtained.

Dr Cheng Wang received his PhD from Beijing Institute of Technology, in 2001. Presently working as a Professor and doctoral supervisor at Beijing Institute of Technology. His research was supported by the National Science Foundation

for Distinguished Young Scholars of China, in 2013. His area of research is explosion mechanics.

In current study, he designed the experiments and numerical methods.

Dr Jianming Yuan received his PhD from University of Science and Technology of China, in 1993. Presently working as principal research scientist in Nanyang Technological University. His area of research is on dynamic behaviour of materials and hydrocode simulation.

In current study he take part in the analysis of experimental results.

Dr Wei Liang Goh received his PhD from Nanyang Technological University, in 2019. Presently working as a research scientist in Nanyang Technological University. His area of research is in armour defeat mechanism study.

In current study, he took part in the analysis of numerical simulation results.

Mr Bin Xu is pursuing his PhD at the Department of Mechanics Engineering of Beijing Institute of Technology. His area of research is explosion mechanics.

In current study he take part in the experimental design and data analysis.